Color separation criteria for spectral multi-ink printer characterization

Binyu Wang (王彬宇)[1,2], Haisong Xu (徐海松)[1*], and M. Ronnier Luo[2]

[1]*State Key Laboratory of Modern Optical Instrumentation, Zhejiang University, Hangzhou 310027, China*

[2]*Department of Colour Science, University of Leeds, Leeds LS2 9JT, UK*

[*]*Corresponding author: chsxu@zju.edu.cn*

Received May 3, 2011; accepted June 3, 2011; posted online August 3, 2011

Seven color separation criteria are evaluated and compared for multi-ink printer characterization, which is a union of five 3-ink and six 4-ink cellular Yule-Nielsen spectral Neugebauer (CYNSN) submodels. In the experimental stage, testing reflectances from printing samples and Munsell color samples are employed. The results show that the prediction and actual accuracy of all the seven selection criteria are approximately the same for printing samples. As for the Munsell samples, the combE_{00} & MI outperforms other selection criteria because it combines one color difference with two metamerism indices, which are important for the heterogeneous samples during prediction.

OCIS codes: 330.1690, 300.6550, 330.1710, 330.1715.

doi: 10.3788/COL201210.013301.

In the printing field, several ways are available for characterizing a multi-ink printer, such as three-dimensional (3D) look-up table and Neugebauer models[1]. However, printing all the required training samples is impossible in some cases because of the ink limit. Chen *et al.*[2] proposed a method to estimate the physically non-realizable cellular primaries of a 6-ink cellular Yule-Nielsen spectral Neugebauer (CYNSN) model[3−6]. Moreover, another method to avoid the ink limit problem is to separate the multi-ink characterization model into several 3- or 4-ink submodels with a selection criterion. Tzeng *et al.* characterized a 6-ink printer by a union of ten 4-ink submodels minimizing metamerism[7].

In terms of selection criteria, several metrics for spectral match quality were introduced in Ref. [8], such as CIE color difference equations, reflectance root mean square (RRMS), weighted RRMS (WRRMS), metamerism index (MI), and so on.

In this letter, a characterization model for a multi-ink printer by a union of five 3-ink and six 4-ink CYNSN submodels is derived. Printing samples and samples from the Munsell book of color are then employed to evaluate the performance of the seven selection criteria, which are minimum CIEDE2000 color difference (ΔE_{00})[9], combined ΔE_{00} (combE_{00}), RRMS, WRRMS, reflectance difference percentage (RDP), combined metamerism index (combMI)[10], and the combination of ΔE_{00} and MI(combE_{00}&MI). The word "minimum" is omitted during comparison of the selection criteria in the discussion stage for simplicity.

For the CMY halftone prints, the classic Yule-Nielsen spectral Neugebauer (YNSN) equation[3,4] is given by

$$r(\lambda) = \Big\{ \sum_{i=1}^{8} a_i [r_i(\lambda)]^{1/n} \Big\}^n, \tag{1}$$

where $r_i(\lambda)$ is the reflectance of the ith primaries at the wavelength λ, a_i denotes the weight of the ith primary, $r(\lambda)$ is the predicted reflectance, and n is the Yule-Nielsen n-factor accounting for the light scattering in the substrate.

One modification that greatly improves the performance of the YNSN model is the cellular technique, which separates the whole color space (e.g., CMY, CMYK) into small subspaces called cells[4]. Taking the CMY as an example, the primaries only have two levels (0 and 1) in the Neugebauer model. If an additional level 0.5 is involved, the CMY color space is divided into 8 subspaces. The Neugebauer model is then implemented in the cell where the testing sample is situated. The CYNSN model combines the YNSN model with the cellular technique, and is easily extended to a higher number of inks.

As mentioned previously, seven selection criteria are exploited in the experimental stage. The first is the CIEDE2000 color difference[9], which is the latest CIE-recommended color-difference formula. CombE_{00} averages three color differences to reduce the metamerism, shown as

$$\text{comb}E_{00} = [\Delta E_{00}(\text{D65}) + \Delta E_{00}(\text{A}) + \Delta E_{00}(\text{F11})]/3, \tag{2}$$

where ΔE_{00}(D65), ΔE_{00}(A), and ΔE_{00}(F11) are the color differences under illuminant D65, A, and F11, respectively.

The RRMS, denotes the degree of spectral match between the two reflectances; however, the value of RRMS depends on the adopted scale of the reflectance. For instance, if the scale of reflectance is in the range of 0 to 1, the corresponding calculated RRMS value ranges from 0 to 1. However, the scale 0–100 is also sometimes used to represent the reflectance values, and the RRMS value becomes 100 times larger. The RRMS can be expressed as

$$\text{RRMS} = \sqrt{\frac{\sum_{\lambda=\lambda_1}^{\lambda_2} [r_1(\lambda) - r_2(\lambda)]^2}{N}}, \tag{3}$$

where $r_1(\lambda)$ and $r_2(\lambda)$ are the predicted and standard reflectances, respectively, and N is the dimensionality of

reflectance. WRRMS can be expressed as

$$\mathrm{WRRMS} = \sqrt{\frac{\sum_{\lambda=\lambda_1}^{\lambda_2} [w(\lambda)\cdot r_1(\lambda) - w(\lambda)\cdot r_2(\lambda)]^2}{N}}, \quad (4)$$

where $w(\lambda)$ is the weight, which is the sum of three CIE color matching functions[8] at each corresponding wavelength in this letter.

Compared to the equal weight at each wavelength for RRMS, WRRMS, given in Eq. (4), takes the human visual property into account. To avoid the scale limitation of RRMS, the RDP is also employed as

$$\mathrm{RDP} = \frac{1}{N}\sum_{\lambda=\lambda_1}^{\lambda_2} \left|\frac{r_1(\lambda) - r_2(\lambda)}{r_2(\lambda)}\right| \times 100\%, \quad (5)$$

which represents the percentage of reflectance change.

Metamerism[10] is the phenomenon wherein two samples with different reflectances match under one set of viewing conditions, but fail to match under another set of conditions. The degree of metamerism is commonly represented by the MI. The combMI in this study is demonstrated by

$$\mathrm{combMI} = [\mathrm{MI(D65A)} + \mathrm{MI(D65F11)}]/2, \quad (6)$$

where MI(D65A) and MI(D65F11) are the special indices of metamerism[8] between illuminant D65 and A, and that between D65 and F11, respectively. And the equation to obtain the combMI & ΔE_{00} is shown as

$$\begin{aligned}\mathrm{comb}E_{00}\&\ \mathrm{MI} =& [\Delta E_{00}(\mathrm{D65}) + \mathrm{MI(D65A)} \\ &+ \mathrm{MI(D65F11)}]/3. \end{aligned} \quad (7)$$

In the experimental stage, the photo printer (Designjet Z3200ps, HP, USA) and premium instant-dry satin photo paper (HP, USA) were used. Eight inks were adopted: grey (Gy), photo black (K), light cyan (C), magenta (M), yellow (Y), chromatic red (R), green (Gn), and blue (B). Based on the location of inks in the a*b* plane of the CIELAB space shown in Fig. 1, ten submodels were selected, containing CMY, RMY, CGnY, CMB, RGB, and their corresponding 4-ink submodels, with the extra ink K.

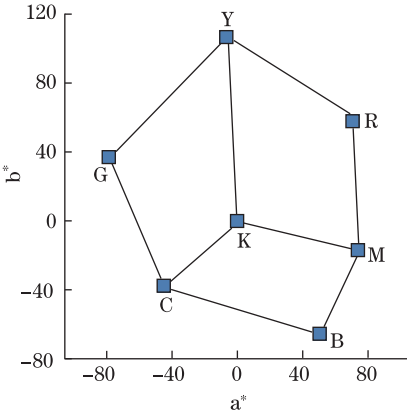

Fig. 1. Locations of the seven inks, except for grey, in the a*b* plane.

Moreover, the CMYGy was also included because of the higher reflectance values of Gy compared to those of K. Each ink was divided into seven levels with approximately the same CIE lightness (L*) interval, resulting in 343 (7^3) and 2 401 (7^4) training samples for every 3- and 4-ink submodel, respectively. In total, 14 406 (6×7^4, 4-ink submodels included corresponding 3-ink submodels with K equal to 0) training samples were generated.

To evaluate the performance of forward submodels, which predict reflectance using Eq. (1) in the located cell for the recipe (digital input for each ink to print), 1 700 testing samples ($5 \times 100 + 6 \times 200$, 100 for each 3-ink submodels, 200 for each 4-ink submodel) were produced using the following procedure. Firstly, to avoid the same digital inputs as training samples, six levels of each ink were interpolated from the corresponding seven levels by averaging two neighboring inks. Secondly, 100 and 200 samples were randomly selected from the 216 (6^3) and 1 296 (6^4) testing samples for each 3- and 4-ink submodel. In the backward model that generates the recipe for the input reflectance, 333 reflectances of printing samples were randomly selected from the 1 700 testing samples above. Together with 330 reflectances of Munsell samples with hues equal to 5R, 5YR, 5Y, 5GY, 5G, 5BG, 5B, 5PB, 5P, and 5RP, these reflectances were set as the standard reflectances to test the accuracy of selection criteria. In addition, all printed samples in the experiment were measured using a GretagMacbeth Spectrolino spectrophotometer, and the spectral range from 400 to 700 nm with a 10-nm interval was recorded. The color difference ΔE_{00} was computed under a 10° standard observer.

Table 1 shows the performance of 11 forward submodels between the measured reflectances of the 1 700 testing samples and their corresponding predicted ones with the YN n-factor set at a typical value of 2.5. In general, every submodel achieves a reasonable accuracy, especially the 3-ink submodels. All the values of MI in Table 1 are less than 0.5. Nonetheless, RGnB, CMYK, CGnYK, and RGnBK performed relatively poorly, with the ΔE_{00} near to or larger than 1. Additionally, the data listed in all the tables in this letter are the average values.

Table 1. Accuracy of 11 Forward CYNSN Submodels

Submodels	ΔE_{00} (D65)	ΔE_{00} (A)	ΔE_{00} (F11)	RRMS	RDP	MI (D65A)	MI (D65F11)
CMY	0.62	0.60	0.64	0.0044	3.15	0.29	0.24
RMY	0.81	0.69	0.78	0.0048	5.97	0.31	0.25
CGnY	0.59	0.59	0.50	0.0075	3.93	0.40	0.34
CMB	0.41	0.45	0.43	0.0033	2.63	0.24	0.20
RGnB	1.02	0.91	0.97	0.0034	4.85	0.39	0.25
CMYK	1.04	1.07	1.04	0.0029	4.90	0.49	0.39
RMYK	0.65	0.62	0.66	0.0023	4.27	0.22	0.17
CGnYK	1.07	1.13	1.11	0.0049	10.78	0.36	0.22
CMBK	0.45	0.45	0.47	0.0019	4.46	0.12	0.11
RGnBK	1.28	1.25	1.28	0.0041	9.89	0.34	0.22
CMYGy	0.59	0.55	0.61	0.0034	4.32	0.20	0.17

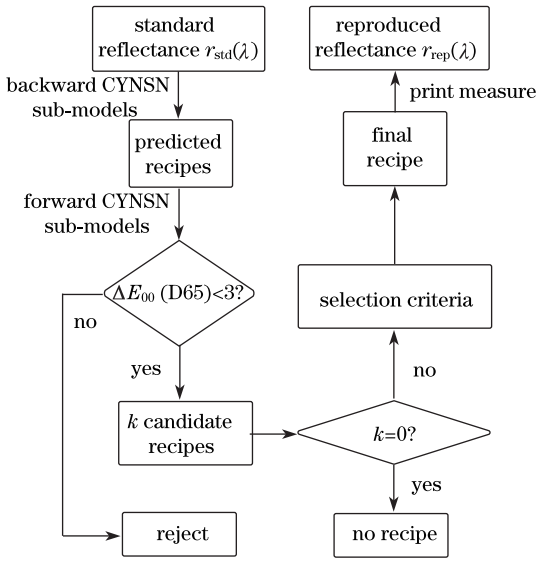

Fig. 2. Flowchart for performing the selection criteria.

The backward CYNSN model is solved by the iteration. In the present study, the linear regression iteration[11] was exploited to reverse the YNSN model, together with QR decomposition[12] to further reduce the computational cost. Meanwhile, the cell searching method proposed by Guo[13] was employed to seek the optimal cell, within which the most accurate recipe could be obtained by implementing the backward YNSN model.

Figure 2 illustrates the flowchart to evaluate the performance of the proposed selection criteria. For any input standard reflectance $r_{\rm std}(\lambda)$, the 11 backward submodels are implemented to obtain the 11 corresponding recipes. Afterwards, the reflectances of the 11 recipes are predicted by the corresponding forward submodels. The predicted ΔE_{00}(D65) is then computed between the predicted and standard reflectances. When the predicted ΔE_{00}(D65) is less than a predetermined threshold, which is set at 3 for this experiment, the corresponding recipe is selected as the candidate recipe. For example, k candidate recipes are obtained. If k is not equal to 0, different selection criteria are implemented to select the final recipe, such as choosing the one having the minimum predicted ΔE_{00}(D65). Otherwise, no recipe is found for the $r_{\rm std}(\lambda)$. Finally, the final recipes are printed and measured, and the actual performance is evaluated between the reproduced and standard reflectances.

Table 2 demonstrates the prediction accuracy of the selection criteria between the predicted reflectances of final recipes and their corresponding $r_{\rm std}(\lambda)$. Clearly, all seven selection criteria have the ability to accurately predict the printing samples. This reveals that the accuracy of the iteration and cell searching method in the CYNSN inversion is excellent, with all mean ΔE_{00} approximately equal to 0.2, which is not surprising because the inks used to print the final recipes are exactly the same as those generating the standard printing reflectances.

In terms of the Munsell samples, the combE_{00} and combE_{00} & MI in the bold font outperform other five because they make a compromise under several illuminants. The reason for the relatively poor performance of the spectral-based selection criteria is that they are not directly optimized for color difference under different illuminants because they assign the same value despite having different weights to every wavelength during the calculation.

Table 2. Prediction Accuracy of the Seven Selection Criteria

Selection Criteria	ΔE_{00} (D65)	ΔE_{00} (A)	ΔE_{00} (F11)	RRMS	RDP	MI (D65A)	MI (D65F11)
Printing Samples							
Min ΔE_{00}(D65)	0.16	0.20	0.21	0.0022	2.02	0.19	0.22
Min combE_{00}	0.17	0.16	0.19	0.0018	1.63	0.15	0.19
Min RRMS	0.18	0.17	0.20	0.0016	1.56	0.15	0.18
Min WRRMS	0.18	0.17	0.20	0.0017	1.56	0.14	0.18
Min RDP	0.18	0.17	0.20	0.0016	1.53	0.15	0.18
Min combMI	0.18	0.17	0.20	0.0016	1.57	0.14	0.17
Min combE_{00}&MI	0.17	0.17	0.19	0.0016	1.56	0.14	0.17
Munsell samples							
Min ΔE_{00}(D65)	0.97	2.02	2.30	0.0420	16.08	2.37	2.95
Min combE_{00}	1.13	1.57	1.79	0.0373	13.94	1.99	2.44
Min RRMS	1.48	1.88	2.20	0.0333	12.51	1.83	2.29
Min WRRMS	1.40	1.90	2.16	0.0354	13.26	1.83	2.22
Min RDP	1.46	1.86	2.18	0.0335	12.38	1.84	2.32
Min combMI	1.45	1.90	2.18	0.0358	13.56	1.61	2.04
Min combE_{00}&MI	1.17	1.74	1.98	0.0369	13.80	1.71	2.12

Based on the above arguments, the final recipes selected via combE_{00} and combE_{00} & MI were printed to test the actual performance of these two selection criteria. As shown in Table 3, the actual accuracy of combE_{00} and combE_{00} & MI is approximately the same, especially for the printing samples. However, compared to combE_{00}, the combE_{00} & MI having lower MI values achieves a better performance for the Munsell samples because the MI is more important for heterogeneous samples during prediction.

To analyze the line between the accuracy and color regions, L* and chroma (C*) are roughly divided into three ranges (i.e., low, middle, and high) and the hue angle (h) has four ranges, which are detailed in Table 4. Figures 3 and 4 illustrate the actual performance (average ΔE_{00} and MI) of combE_{00} & MI in the 36 (3 × 4 × 3) color regions denoted by C*/h/L* in the sequence, whereas that of the combE_{00}, which is not shown, has

Table 3. Actual Accuracy of CombE_{00} and CombE_{00}&MI

Selection Criteria	ΔE_{00} (D65)	ΔE_{00} (A)	ΔE_{00} (F11)	RRMS	RDP	MI (D65A)	MI (D65F11)
Printing Samples							
Min combE_{00}	1.65	1.61	1.62	0.0096	11.01	0.48	0.44
Min combE_{00}&MI	1.67	1.64	1.65	0.0098	11.17	0.46	0.43
Munsell Samples							
Min combE_{00}	1.72	2.19	2.39	0.0386	15.09	2.01	2.44
Min combE_{00}&MI	1.79	2.34	2.55	0.0382	14.93	1.75	2.14

Table 4. Ranges for Lightness, Chroma, and Hue Angle

No.	C*	h	L*
1	0–35 (low C)	315°–45° (Rh)	0–35 (low L)
2	35–70 (mid C)	45°–135° (Yh)	35–70 (mid L)
3	70–100 (high C)	135°–225° (Gh)	70–100 (high L)
4		225°–315° (Bh)	

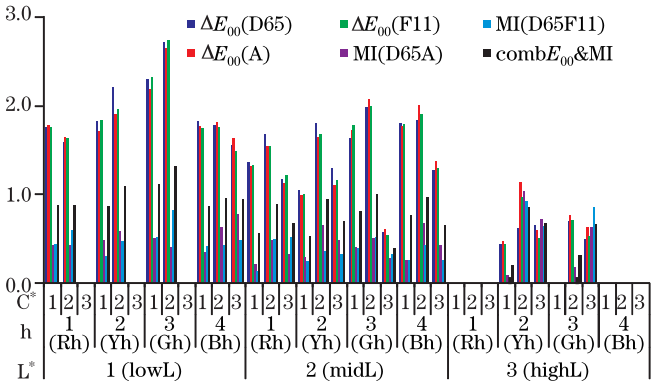

Fig. 3. Actual performance of combE_{00}&MI in color regions for Printing samples.

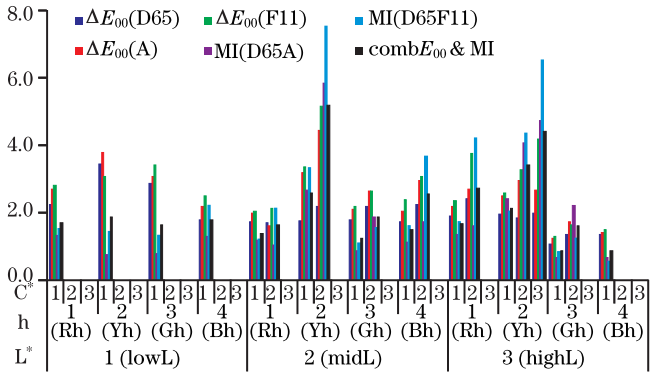

Fig. 4. Actual performance of combE_{00}&MI in color regions for Munsell samples.

the same trend.

As shown in Fig. 3, although some color regions, especially those with high C*/low L* and high C*/high L*, have no sample, only a few real surface colors are located in these regions. The phenomenon can also be observed in Fig. 4. Except for the samples in the color regions of 2(midC)/2(Yh)/1(lowL), 1(lowC)/3(Gh)/1(lowL), and 2(midC)/3(Gh)/1(lowL), the three actual color differences in other regions are close to or less than 2. Moreover, only 16% (54 out of 330) of the printing samples lie in the above three-color regions with low L*.

With regard to Munsell samples, Fig. 4 shows that the values of MI are extremely large for some samples, which is why MI becomes more important for heterogeneous samples during prediction. The actual accuracy of 19 samples located in the color regions of 2(midC)/2(Yh)/2(midL), and 3(highC)/2(Yh)/3(highL) are relatively poor, especially for MI values.

Meanwhile, most of the 14 Munsell samples without recipes using the procedure in Fig. 2 are yellowish color, with high L*, and middle or high C*. These indicate that the CYNSN submodels may not accurately predict the yellowish Munsell samples with relatively high C* and L* in this study. One likely reason is that there are only a few printed training samples in the high C* and L* regions, which are difficult to generate using the printer and are infrequently used in common applications. In general, the combE_{00} & MI works well for most of the printing and Munsell testing samples.

In conclusion, the multi-ink printer characterization is derived using a union of five 3-ink and six 4-ink CYNSN models in this letter. Seven color separation criteria based on the metrics for spectral match quality are evaluated and compared for the testing reflectances of printing and Munsell samples. The prediction and actual accuracy of the seven selection criteria are close to that of printing samples, revealing that the linear regression iteration and cell searching method of the backward CYNSN model worked excellently. As for Munsell samples, the combE_{00} & MI outperformed other selection criteria because one color difference is combined with two metamerism indices, which are important for the heterogeneous samples during prediction. Except for a small percentage of printing samples with low L* and yellowish Munsell samples with relatively high C* and L*, the combE_{00} & MI performs well for most printing and Munsell testing samples.

This work was supported by the Clariant Asia Trainee Program.

References

1. G. Sharma, *Digital Color Imaging Handbook* (CRC, New York, 2003).
2. Y. Chen, R. S. Berns, and L. A. Taplin, J. Imag. Sci. Tech. **48,** 6 (2004).
3. D. Wyble and A. Kraushaar, Col. Res. Appl. **30,** 322 (2005).
4. D. R. Wyble and R. S. Berns, Col. Res. Appl. **25,** 4 (2000).
5. J. Guo, H. Xu, and M. R. Luo, Chin. Opt. Lett. **8,** 1106 (2010).
6. B. Wang, H. Xu, M. R. Luo, and J. Guo, Chin. Opt. Lett. **9,** 063301 (2011).
7. D. Tzeng and R. S. Berns, in *Proceedings of Color Imaging Conference 8* 342 (2000).
8. F. H. Imai, M. R. Rosen, and R. S. Berns, in *Proceedings of European Conference on Colour in Gaphics, Imaging, and Vision 2002* 492 (2002).
9. M. R. Luo, Rev. Prog. Color **32,** 28 (2002).
10. G. Wyszecki and W. S. Stiles, *Color Science*: *Concepts and Methods, Quantitative Data and Formulae* (Wiley, New York, 2000).
11. P. Urban and R. R. Grigat, Col. Res. Appl. **31,** 229 (2006).
12. C. Li and M. R. Luo, in *Proceedings of Color Imagine Conference 16* 84 (2008).
13. J. Guo, "Developing the inverse spectral-based Neugebauer equations", Master Thesis (University of Leeds, 2009).